Preliminary Development and Evaluation of Lightning Jump Algorithms for the Real-Time Detection of Severe Weather

Christopher J. Schultz * and Lawrence D. Carey

The University of Alabama in Huntsville, Huntsville, Alabama

Walter A. Petersen

NASA MSFC, Huntsville, Alabama

ABSTRACT

In the past decade, several studies have shown that rapid increases in total lightning activity (intracloud + cloud-to-ground) have been observed several minutes in advance of the occurrence of severe weather at the ground. These rapid increases in lightning activity have been termed "lightning jumps." Encouragingly, a positive correlation between lightning jumps and the manifestation of severe weather at the ground have also been documented in thunderstorms occurring across the Tennessee Valley. This study examines several lightning jump algorithms, including the algorithm proposed by Gatlin (2006), in order to move forward on the development of an operationally-applicable jump algorithm that can be used with either total lightning observations made on the ground, or in the near future from space (e.g., the GOES-R Geostationary Lightning Mapper; GLM).

1. Introduction

Numerous studies have demonstrated the usefulness of total lightning data as it pertains to severe weather situations (Goodman et al. 1988, MacGorman et al. 1989, Williams 1989a, Williams et al. 1999, Buechler et al. 2000, Goodman et al. 2005, Bridenstine et al. 2005, Wiens et al. 2005, Steiger et al. 2005, Gatlin 2006, Steiger et al. 2007). Countless positive correlations are made in these studies between rapid increases in total lightning, also termed *lightning jumps* (Williams et al. 1999), and manifestations of severe weather at the surface. Of course not all severe weather is preceded by a lightning jump, nor do all storms that produce these rapid increases in lightning contain severe weather. Yet, despite occasional ambiguities, numerous concrete examples of increases in lightning several minutes prior to severe weather have been observed in thunderstorms across Alabama, Tennessee, Florida, Texas, Oklahoma and Colorado.

Thunderstorm electrification is primarily due to non-inductive charging (NIC; Takahashi 1978, Saunders et al. 1991. NIC is any charging mechanism that does not require the presence of an existing electric field. The primary mechanism for thunderstorm charging is the graupel-ice mechanism, where charge is transferred between ice crystals and graupel particles in the presence of supercooled water. Dye et al. (1989) confirmed that the development of an ice phase within thunderclouds coincides with the electrification of the thunderstorm. The combination of a thunderstorm's updraft and Earth's always present gravitational force allows for charge separation within the cloud, thus forming an electric field within the cloud. As charge continually builds over time, electric breakdown takes place, and lightning occurs.

Workman and Reynolds (1949) showed that the amount of lightning produced by a thunderstorm is closely tied to a thunderstorm's updraft. Vonnegut (1963), Williams (1985), and Boccippio (2002) demonstrated that a nonlinear relationship exists between storm depth and the amount of lightning a storm produces. Thus, thunderstorms that have stronger updrafts (e.g. severe thunderstorms) will have the potential produce more lightning. Petersen et al. (2005) provide strong evidence linking precipitation ice mass to lightning occurrence and amount while Deierling (2006) links the ice mass and updraft to lightning occurrence by demonstrating correlation between the vertical flux of ice and the total flash rate. Therefore, there is a link between the strength of a thunderstorm's updraft, ice fluxes, and the amount of lightning that occurs within a thunderstorm.

The first noteworthy correlation between total lightning rate and storm severity was made visually by Bernard Vonnegut and Charles Moore during a tornadic storm in Massachusetts in 1953. Vonnegut and Moore described the lightning activity as "going like gangbusters" as they watched the storm move off into the Atlantic Ocean (Williams

et al. 1999). In the mid to late 1980's Goodman et al. (1988) and Williams et al. (1989a) correlated total lightning rates to the onset of wet microbursts in Northern Alabama. MacGorman and Rust (1989) also observed increases in total lightning in a tornadic thunderstorm near Binger, Oklahoma in 1981. In the past decade, many studies continued to find similar findings. Williams et al. (1999) found increases in the total flash rate prior to severe weather in several thunderstorms in Florida. Goodman et al. (2005) showed similar results for tornadic thunderstorms in South Central Tennessee, as well as for a damaging microburst case near Huntsville, AL in August of 2002. Wiens et al. (2005) demonstrated that these increases in lightning also occur across the High Plains during the STEPS field project in 2000 (Lang et al. 2004). Wiens as well as Tessendorf et al. (2005, 2007) compared lightning rates to updrafts and graupel/hail volume using dual Doppler analysis. Gatlin (2006) showed once again that lightning jumps occur prior to the onset of severe weather in the Tennessee Valley, and his work utilized the time rate of change of the total flash rate to be used as a predictor to define a jump in the total amount of lightning. Other noteworthy studies can be found from the Dallas total lightning network (e.g., Steiger et al. 2005, Wilson et al. 2006, Steiger et al. 2007).

Gatlin (2006) provided a "strawman" framework for an operational algorithm that could be used by a warning forecaster to assess a storm's severity through the incorporation of total lightning data. Using the time rate of change of the total flash rate, jumps in this derivative of total lightning have been found to precede severe weather at the surface by as much as 25 minutes (Goodman et al. 2005). However, Gatlin did not 1) analyze of total lighting in severe storms other than isolated cases, 2) study total lightning behavior in ordinary non-severe thunderstorms, and how non-severe thunderstorms may affect the performance of an operational algorithm. The first area has significance because not all severe weather producing storms are isolated. This is especially true in the Southeast US, where severe thunderstorms are often embedded within a convective line (Bunkers et al. 2006). Another situation where this may be relevant is during the lifetime of landfalling tropical cyclones, where the outer bands of these storms can produce tornadoes (McCaul 1987, McCaul 1991). The second area of focus is important because all thunderstorms must exhibit at least one jump in lighting activity during their lifetime (i.e., prior to first lightning in the cumulus stage or later impulsive changes associated with pulsing growth in the latter mature and dissipating stages; Byers and Braham (1949)). These pulses in activity conceivably lead to false alarms on thunderstorms that are clearly below severe limits, thus creating a lack of confidence in the operational product.

The purpose of this study is to investigate the link between total lightning and the occurrence of severe weather in a wide range of thunderstorm types. Based on the results, the aim is also to provide a means to improve lead times and forecaster confidence during the warning process, allowing for more timely and accurate warnings. The final goal is to continue the development of an operational algorithm for use in the Geostationary Operational Environmental Satellite Series R (GOES-R) Lightning Mapper data stream (Goodman et al. 2006).

2. Data and Methodology

Severe and non-severe thunderstorms are used to observe electrical activity in all forms of convection. Severe thunderstorms were chosen if they exceeded today's National Weather Service criteria for severe weather of 1) hail $\geq$ 1.9 cm, 2) wind $\geq$ 26 m s^{-1}, 3) or the occurrence of a tornado. All severe weather reports were taken from the National Climatic Data Center's (NCDC) severe weather database. Non-severe thunderstorms were chosen if they 1) lasted for at least 30 minutes, and 2) there was not any reported severe weather with the thunderstorm. Non-severe thunderstorms were limited to the warm season (May-September).

Total lightning data was recorded using two very high frequency (VHF) lightning mapping arrays (LMA; e.g., Rison et al. 1999). LMA source data was clustered into individual flashes using a spatial and temporal clustering algorithm developed by McCaul et al. (2005). Flashes were thresholded at 10 sources or greater to filter out some of the smaller lightning flashes (Wiens et al. 2005). Total lightning data is limited to 150 km, as source location errors increase dramatically beyond this range (Koshak and Coauthors 2004). Cloud-to-ground (CG) lightning data utilized in this study was taken from the National Lightning Detection Network (NLDN; Cummins et al. 2006) and data were thresholded at $\geq +15$ kA (Biagi et al. 2007).

Radar data was acquired from NCDC's archived Level-II database for five National Weather Service (NWS) Weather Surveillance Radar-1988 Doppler (WSR-88D; Crum and Alberty 1993) located at Hytop, AL (KHTX), Calera, AL (KBMX), Columbus Air Force Base, MS (KGWX), Old Hickory, TN (KOHX), and Sterling, VA (KLWX). These radars surround or are centered within the 150 km domain from the center of each LMA. Level-II data was then converted using REORDER, and placed into the Thunderstorm, Identification, Tracking, and Nowcasting (TITAN; Dixon and Wiener 1993 algorithm for tracking purposes. Specific information from each thunderstorm (i.e., location, size) was then used to create cell based interrogations of reflectivity, azimuthal shear, and vertically integrated liquid (VIL) through the use of the Warning Decision Support System-Integrated Information (WDSS-II; e.g., Lak-

shmanan et al. 2006, 2007).

Six lightning jump algorithm configurations were created to test against the sample of thunderstorms. First off, lightning jumps will be determined using the time rate of change of the total flash rate termed DFRDT. The Gatlin and Gatlin 45 algorithms are based on the work of Gatlin (2006). The 2σ and 3σ use the previous ten minutes of lightning data to statistically analyze if the current value of DFRDT is abnormal or not. The Threshold 8 and Threshold 10 algorithms use previously observed total lightning flash rates and DFRDT rates to create hard thresholds to try to delineate between severe and non-severe thunderstorms. After a lightning jump has been signaled, a "severe warning" is placed on the thunderstorm for forty-five minutes.[1]

Observed lightning jumps were counted as a hit if severe weather occurred within the forty-five minute period after the jump. If a jump occurs and there is not reported severe weather in the forty-five minute period after, this is counted as a false alarm. Likewise, if severe weather occurs in the absence of a lightning jump, this is counted as a miss. If multiple jumps occur within a warning period and severe weather is observed while both jumps are valid, the earliest jump is credited with the hit. Probability of detection (POD), false alarm rate (FAR), critical success index (CSI) and Heidke Skill Scores were also calculated for the entire dataset.

3. Results

a. Non-Severe Thunderstorms

1) Non-Severe Thunderstorm Characteristics

Determination of what is "normal" lightning behavior for a thunderstorm must first be considered prior to implementing an algorithm that identifies a storm as severe. For example, the overall sample of sixty-nine non-severe thunderstorms from two different regimes yields an average peak flash rate for non-severe storms of 10.30 flashes min^{-1}. Furthermore, examining the DFRDT characteristics of the non-severe dataset reveals that the average peak DFRDT value of 4.90 flashes min^{-2}. Using the North Alabama cases, 90% of the non-severe thunderstorms fall below a threshold of 8 flashes min^{-2}, while 93% fall below a threshold of 10 flashes min^{-2}, and these two thresholds are the second part of the threshold technique. Importantly the average peak flash rate can be applied to the 2σ, 3σ, and threshold algorithms for initialization. The DFRDT information is then used for creation of a second limit to determine whether or not a lightning jump occurs.

[1]The Gatlin algorithm only has a 30 minute warning to be consistent for comparisons with the work done in Gatlin (2006)

2) Testing of Algorithms on Non-severe Thunderstorms

The next step is to test the non-severe dataset against each of the algorithms to understand potential false alarm rates for misidentification of non-severe storms as severe. Table 1 shows the number of warnings that would be issued on the Northern Alabama dataset for non-severe thunderstorms using each lightning jump algorithm configuration. Leading the way in number of false alarms is the Gatlin methods with 92 falsely identified warnings. The 2σ algorithm produced 16 false alarms for the non-severe dataset, and the 3σ came in with slightly fewer with 10 false alarms. The threshold algorithms performed best in not misclassifying non-severe thunderstorms as severe using total lightning data. The Threshold 8 algorithm identified 7 false alarms, and the Threshold 10 only identified 6 false alarms for the non-severe sample.

b. Severe Thunderstorms

1) Case Examples

(i) 4 April 2007, MCS

After thunderstorms dropped large hail across the Tennessee Valley during the afternoon hours on 3 April 2007, a large MCS moved into the Tennessee Valley from the northwest during the late evening hours. This system developed in the Mid Mississippi Valley during the early afternoon on 3 April and plowed southeastward ahead of a strong cold front. Severe weather was already ongoing as the complex entered the domain of study. Using the 35 dBZ at -15°C isolation technique, several thunderstorm cells are identified within the convective line.

One thunderstorm formed just to the north of the AL/TN border in Pulaski and Giles County, TN about 0245 UTC on April 4, 2007. This cell was located just ahead of the main MCS squall line that had produced severe hail and wind across Central Tennessee. Initially, total flash rates were only on the order of 10 min^{-1}, and the maximum height of the 35 dBZ contour was consistently found between 10 and 11 km (Figure 2). The MCS approached the area from the northwest and interacted with the developing storm about between 0300 and 0310 UTC. Coincident with the collision between the developing cell and convective line, the 35 dBZ height shot upward to 13 km around 0306 UTC. In response to the vertical growth and interaction with the bow echo, the total flash rate for the storm dramatically jumped from 23 flashes min^{-1} at 0257 UTC to 87 flashes min^{-1} at 0310 UTC (Figure 2). During this period all six algorithms triggered for this area. Around 0325 UTC a small EF0 tornado occurred near Taft, TN. This tornado then moved across the AL/TN state line and dissipated near the town of Hazel Green, AL. The report

was not received by the NWS Huntsville until 0340 UTC, which demonstrates the problematic nature of severe weather event report times. Around 0330 UTC, a 65 dBZ maximum in reflectivity formed around 5 km and dipped down to the surface. At 0335 UTC several power poles were snapped off at the base near Maysville AL, and at 0345 UTC 1.00 inch hail was reported in Flintville, TN. Again, it is emphasized that on average the lightning jump for this case occurred nearly 30 minutes in advance of the manifestation of severe weather at the surface.

(ii) 25 September 2005, Tropical Cyclone Tornado

On September 23, 2005, Hurricane Rita made landfall along the southeast coast of TX producing significant damage along this stretch of the Gulf Coast. By September 25, 2005, the remnants moved into Central and Northern AL, and the system's outer bands produced several severe thunderstorms. One such thunderstorm spawned two tornadoes near Double Springs, AL. The severe thunderstorm that spawned the tornadoes initially developed outside of the maximum range set for this study (>150 km); however, by 1844 UTC the storm moved into the outer 150 km domain. Total flash rates for this storm were low at 1844 UTC (1-2 min^{-1}), which is expected for thunderstorms associated with tropical systems. At 1848 UTC the Gatlin algorithm sounded an alarm due to a slight increase in 1 minute averaged flash activity, showing that the Gatlin algorithms are sensitive to small changes in flash rate. The lightning flash rate at this point increased from 1 flash min^{-1} to 2 flashes min^{-1}. From 1844 UTC to 1915 UTC, the vertical extent of the thunderstorm remained constant, with the 35 dBZ height extending up to 8 km, and the 50 dBZ height remaining around 5 km. However, the rotational velocity of the storm increased in the lowest levels of the thunderstorm. Azimuthal shear values noticeably increased for the next 50 minutes, with values ranging from $4x10^{-3}$ s^{-1} to $6.5x10^{-3}$ s^{-1}. This rotation was confined to the lowest 3 km of the storm.

Looking at Figure 3, around 1920 UTC a 55 dBZ core developed aloft near a height of 4 km. By 1930 UTC the core extended up to 5 km and the 35 dBZ echo top height reached up to the 9 km height. Increases in height shown in the time-height plot (Figure 3) along with higher reflectivity values indicate that there were larger amounts of ice present aloft. In response to the vertical growth the total flash rate increased from 1 flash min^{-1} at 1923 UTC to 10 flashes min^{-1} by 1927 UTC. At this time the 10 flash threshold was met and four of the six algorithms warn on this potentially dangerous cell. Between 1943 UTC and 1948 UTC, the CG flash rate peaks at 3 CG flashes min^{-1}, all comprising of negative flashes. At 1954 and 1957 UTC two tornado reports are relayed to the National Weather Service in Birmingham, and a tornado warning was issued.

c. Summary of Datasets

Presented here are the results for the entire dataset of thunderstorms studied. Statistical methods are applied to the dataset to evaluate the performance of each individual algorithm. POD, FAR, CSI and a Heidke Skill Score are determined for each algorithm, broken down by range from the individual LMA center.

1) The Gatlin Algorithms

Referring to Table 2 and Table 3, the Gatlin and Gatlin 45 algorithms display a high POD (0.8922 and 0.9804 respectively); however, their FAR is also high, with values at 0.4204 and 0.5780 solely for severe thunderstorms. As discussed multiple times during the case study descriptions, the Gatlin algorithm is easily triggered through small changes in the total flash rate. When non-severe thunderstorms are added to the sample set, the FARs for these two algorithms swell to 0.6286 and 0.6169. The CSI values just for the severe set are quite strong with values between 0.48 and 0.54; however, once again when the non-severe thunderstorm dataset is combined, the CSI drops by nearly a third. Comparing the Gatlin algorithm with 30 minutes of warning length to values presented in Gatlin (2006), the POD is nearly 0.08 higher Gatlin's original results while CSI is similar at 0.549. Unfortunately, high FAR values outshine the high POD results, so this algorithm configuration would need some additional improvements.

2) The Sigma Algorithms

The 2σ algorithm is another "black box" method that shows promise in the detection of severe weather using lightning trend data. Looking at Table 4, the POD for this algorithm at ranges closer than 100 km is around 0.8725. The FAR for severe thunderstorms is an impressive 0.2583; however, if non-severe thunderstorms are included, the FAR increases to 0.3456. CSI is slightly higher than the Gatlin algorithms at 0.6692, and only falls slightly to 0.5973 if the non-severe dataset is included. Heidke Skill Scores are very high with a score of 0.8018 and 0.7479 for the severe and entire dataset. Considering that a perfect Heidke Skill Score is 1, the above metrics suggest that the 2σ method is a relatively robust algorithm.

3σ results are not as promising as the 2σ algorithm. Comparing Table 4 and Table 5, the POD decreases, reaching a value of 0.4902 and CSI near 0.4425. FAR is the lowest of the algorithms at 0.1803 at 100 km or shorter, but this would not help if the algorithm is missing half of the severe weather events. The decrease in POD and FAR are expected as 3σ algorithm has a slightly higher jump

threshold than the 2σ method. Looking once again at Table 5, little if any improvement is found as the domain is extended to 150 km, and the increase in POD may be in part to an increase in the number of severe events. Heidke Skill Scores hover near a respectable 0.6000, but the main issue with this algorithm is the POD.

3) The Threshold Algorithms

The threshold based methods also show some promise for severe weather applications. Results presented in Tables 6 and 7 show that these simple threshold-based approaches yield POD values at 0.7553 for the Threshold 10 method, and 0.8039 for the Threshold 8 method. False alarms are manageable for both algorithms, as FARs are 0.2991 and 0.3740 when applied to the entire dataset. As range increases, values of POD, FAR and CSI increase slightly, and this once again may be attributed to the increase in the number of severe events. Heidke Skill Scores are up around 0.70 for both algorithms at either range, once again indicating promise for severe weather application.

4. Discussion

The primary objectives of this study were to

i. Identify severe and non-severe thunderstorms in a variety of environments and settings.

ii. Gain insight into non-severe thunderstorm total lightning behavior (flash rates, changes in flash rate).

iii. Apply the knowledge gained from the non-severe dataset to develop lightning jump algorithms for the detection of severe weather to improve upon the "strawman" implemented in Gatlin (2006)

Analysis of the non-severe dataset reinforces what we already know from other studies about average flash rate. Livingston and Krider (1978) presented that an ordinary non-severe thunderstorm has an average peak flash rate near 10 flashes min^{-1}. Using the results from this study, we have reaffirmed that the average peak flash rate for a non-severe thunderstorm was 10 flashes min^{-1}. This information is then implemented in the algorithms developed by this study to reduce the number of false alarms.

The Gatlin algorithms had a high POD (Gatlin: 0.8922, Gatlin 45: 0.9766; Tables 2 and 3); however, this is due to the fact that the algorithms warned on nearly every increase in total lightning. The FAR for both algorithms were very high, with the original Gatlin algorithm at 0.6283 and 0.6169 respectively. In turn, CSI values were low due to the high FAR, dipping down near 0.3750. This algorithm failed miserably in non-severe situations, where there was an average of 2.1 false warnings for the 43 non-severe thunderstorms in North Alabama.

The 2σ algorithm performed the best when compared to the other lightning jump algorithms in this study. The 2σ algorithm had a high POD near 0.8725 and a FAR value of 0.3456 when tested against the entire storm dataset (see Table 4). Heidke Skill Scores approach 0.75, with a value of 1 being perfect. Positively this algorithm worked in complex weather situations; however, more thunderstorm events must be tested to determine the flexibility of the algorithm.

The 2σ performed very well on most of the thunderstorms in this dataset. The 10 flash min^{-1} requirement to initiate the algorithm showed positive results because the 2σ eliminated most smaller jumps that occurred with non-severe convection and time periods where severe storms were below severe criteria. Additionally, the FAR for the overall population sample is lower when compared to NWS FAR statistics from 2003 (Barnes et al. 2007). POD is high, with values between 0.87 and 0.89 depending on range.

The 3σ algorithm performed poorly in severe weather situations. Referring to Table 5, the POD for this algorithm was only around 0.50. False alarm rate statistics were the lowest of the group of algorithms at 0.25; however, the lack in POD is the downfall of this algorithm. Despite the lower POD, HSS values are around 0.60 with indicate that there is some value to this method. Furthermore, the results from the 3σ method can be used to further refine the 2σ algorithm, because this threshold acts as an upper bound for future work.

The Threshold algorithms also provide some promising results (see Tables 6 and 7). The POD values for the Threshold 8 algorithm (Table 7) were around 0.80 and false alarm rates were only near 0.3740 using severe and non-severe thunderstorms. This algorithm performs well in situations where flash rates are high, but not in situations where flash rates are lower and less variant. The Threshold 10 algorithm (Table 6) performed very well too, with POD values near 0.7353 and FAR values as low as 0.3363. The Threshold 10 algorithm also suffers in low flash rate and in situations where the flash rate does not vary considerably. In any case, the 2σ approach yielded higher results.

Overall, the use of lightning jump algorithms on many different types of thunderstorms shows that the lightning jump algorithms have the potential to indicate storm severity regardless of environment. This shows promise that there is potential to track severe weather amongst different storm types confined in the GOES-R FOV. However, we must further test the lightning jump algorithms in other areas of the country to confirm that similar results can be found using any of the lightning jump algorithms presented

here, most specifically, the 2σ algorithm.

5. Conclusions

Sixty-nine non-severe thunderstorms were used to determine what normally occurs within ordinary convection. An average 1 minute peak flash rate from the sample is found to be just below 10 flashes min^{-1}, similar to what past studies have found in Florida (e.g., Livingston and Krider 1978). An average DFRDT rate for this same dataset is near 4.90 flashes min^{-2}. Although this number is not used in any of the proposed algorithms, this may be a useful number in the future if a lower bound greater than zero needs to be applied to define the end of a jump. DFRDT rates at the 90 and 93% level of the non-severe sampling distribution are also found to be at 8 flashes min^{-2} and 10 flashes min^{-2}, respectively. The average peak flash rate information is used to define a lower limit that the flash rate has to reach for the 2σ, 3σ, Threshold 8 and Threshold 10 algorithms to initalize. Furthermore, the peak DFRDT rate information acts as a second level of security for the alarm to sound for the Threshold 8 and Threshold 10 algorithms. Importantly, the behavior of the general population is used to identify non-standard, or "severe" behavior.

Of the sixty-nine thunderstorms, all forty-seven North Alabama cases were tested against each algorithm to see how many false alarms were triggered in situations where storms remain below severe limits. The Gatlin (2006) algorithms performed poorly, with 92 false alarms identified solely in the non-severe database. This is due to the high sensitivity of the algorithm to small increases in total flash rate. The 2σ algorithm performed much better with 16 false alarms triggered, followed by the 3σ with 10, Threshold 8 with 7 and rounding out the bottom the Threshold 10 with 6 false alarms. This information was then incorporated into the statistics after the severe sample is tested.

Severe thunderstorms were broken down by range to see if distance from the center of the LMA had any influence on lightning algorithms. At 100 km, 35 severe thunderstorms with a total of 101 severe weather events were tested against each algorithm. At a range of 150 km, 38 severe thunderstorms were tested with a total of 126 severe weather events. The severe dataset ranges in storm type from isolated supercells to tornadic cells in tropical storm remnants, and all types of severe weather is represented. Several useful results were noted, and weaknesses of each algorithm were highlighted.

The Gatlin algorithm with a 30 minute warning length had a POD of 0.8922, a FAR of 0.6286, CSI near 0.3555, and a Heidke Skill Score of 0.5245 within a 100 km range of the LMA center (Table 2). The numbers remain constant with range (POD 0.8984, FAR 0.6384, CSI 0.3474, HSS 0.5157). The version of Gatlin with a 45 minute warning length had a higher POD, but at the same time a higher FAR. The Gatlin 45 algorithm resulted in POD, FAR, CSI and HSS values within 100 km of 0.9804, 0.6169, 0.3802 and 0.5157, respectively (Table 3). Extending out to 150 km, these values were once again nearly the same with the POD at 0.9766, the FAR at 0.6201, the CSI near 0.3765 and a HSS of 0.5470. Part of the reason for high false alarm rates associated with the Gatlin algorithm is its high sensitivity to small changes in flash rate. Therefore the algorithm warned on nearly every increase in lightning activity.

The 2σ algorithm at 100 km had a POD 0.8725, a FAR of 0.3456, a CSI at 0.5973, and a HSS of 0.7479 (Table 4). Values at 150 km once again nearly mimicked the 100 km results with POD near 0.8984, a FAR of 0.3466, the CSI at 0.6085, and a HSS of 0.7566. This simple approach yielded significant results for detection of severe weather using total lightning data. The POD value was high while false alarm rates are much lower than the Gatlin algorithms. The CSI value was also significantly higher than the Gatlin algorithms, and Heidke Skill Score was strong, at nearly 0.75.

The 3σ algorithm performs the poorest with POD values at 0.4902, the FAR near 0.2958, CSI at 0.4065 and a HSS of 0.5780 (Table 5). Slight improvement occurs when the domain is extrapolated out to 150 km with numbers showing a POD of 0.5156, a FAR of 0.2584, a CSI at 0.4681, and a HSS at 0.6083. These results were not as robust as the 2σ configuration, and this was due to the higher jump threshold. Although the algorithm demonstrated a low FAR, the POD was not as high as the previous algorithms.

The numbers for Threshold 10 algorithm were as follows: POD 0.7353, FAR at 0.3363, CSI 0.5357, HSS 0.6977 (Table 6). The Threshold 8 algorithm has slightly higher numbers with a POD of 0.8039, a FAR at 0.3740, a CSI at 0.5430, and a HSS of 0.7039 (Table 7). Both threshold methods show slight improvement out to 150 km, but this may only be attributed to an increase in the number of severe events. Values for the Threshold 10 algorithm at 150 km are 0.7578, 0.3533, 0.5359, 0.6978 (POD, FAR, CSI, HSS), while the numbers for the Threshold 8 algorithm are 0.8281, 0.3908, 0.5408, 0.7020. This is another relatively simple method that showed promise. POD was not as high as the 2σ or Gatlin algorithms, but Heidke Skill Scores demonstrate that there was skill involved in these two methodologies. This algorithm was simple because it takes the most recent period of data only to see if a thunderstorm had reached severe limits. No previous history of the thunderstorm was needed at any point in time. The algorithms had problems in situations where low flash rates or low variability in the flash rate kept the algorithms dormant.

Overall, there is high potential for a lightning jump algorithm for use in severe weather operations. Currently

the 2σ configuration demonstrates the highest promise for such an algorithm; however, improvements are always possible. The number of cases for both severe and non-severe thunderstorms must be increased to converge on a line to delineate between severe and non-severe thunderstorms. Data from other regions of the country must also be tested against these algorithms to see if there is any regional dependence that would raise or lower the ability to detect severe weather. Collection of these cases into a database would then be used to apply probability statistics to help separate severe and non-severe thunderstorms as best as possible as well as to further test the the lightning jump algorithms performance.

REFERENCES

Barnes, L. R., E. C. Gruntfest, M. H. Hayden, D. M. Schultz, and C. Benight, 2007: False alarms and close calls: a conceptual model of warning accuracy. *Wea. and Forecasting*, **22**, 1140–1147.

Biagi, C. J., K. L. Cummins, K. E. Kehoe, and E. P. Krider, 2007: National Lightning Detection Network (NLDN) performance in southern Arizona, Texas and Oklahoma in 2003-2004. *J. Geophys. Res.*, **112**, doi: 10.1029/2006JD007341.

Boccippio, D. J., 2002: Lightning scaling relations revisited. *J. Atmos. Sci.*, **59**, 1086–1104.

Bridenstine, P. V., C. B. Darden, J. Burks, and S. J. Goodman, 2005: The application of total lightning data in the warning decision making process. *Preprints, Conf. on the Meteor. Appl. of Lightning Data*, San Diego, CA, Amer. Meteor. Soc.

Buechler, D. E., K. T. Driscoll, S. J. Goodman, and H. J. Christian, 2000: Lightning activity within a tornadic thunderstorm observed by the Optical Transient Detector (OTD). *Geophys. Res. Lett.*, **27**, 2253–2256.

Bunkers, M. J., M. R. Hjelmfelt, and P. L. Smith, 2006: An observational examination of long-lived supercells. Part I: Characteristics, evolution, and demise. *Wea. and Forecasting*, **21**, 673–688.

Crum, T. D. and R. L. Alberty, 1993: The WSR-88D and the WSR-88D Operational Support Facility. *Bull. Amer. Meteor. Soc.*, **74**, 1669–1687.

Cummins, K. L., J. A. Cramer, C. J. Biagi, E. P. Krider, J. Jerauld, M. A. Uman, and V. A. Rakov, 2006: The US National Lightning Detection Network: Post-upgrade status. *Preprints, 2nd Conf. on Meteorological Applications of Lightning Data*, Atlanta, GA, Amer. Meteor. Soc., CD-ROM, 6.1.

Deierling, W., 2006: *The Relationship Between Total Lightning and Ice Fluxes*. Ph.D, University of Alabama-Huntsville, 175 pp.

Dixon, M. and G. Wiener, 1993: TITAN: Thunderstorm Identification, Tracking Analysis and Nowcasting-A radar-based methodology. *J. Atmos. Ocean Tech.*, **10**, 785–797.

Dye, J. E., W. P. Winn, J. J. Jones, and D. W. Breed, 1989: The electrification of New Mexico thunderstorms. 1. Relationship between precipitation development and the onset of electrification. *J. Geophys. Res.*, **94**, 8643–8656.

Gatlin, P., 2006: *Severe Weather Precursors in the Lightning Activity of Tennessee Valley Thunderstorms*. M.S. Thesis, University of Alabama-Huntsville, 87 pp.

Goodman, S. J., R. Blakeslee, H. Christian, W. Koshak, and W. A. Petersen, 2006: GOES-R Lightning Mapper (GLM) research and applications risk reduction. *Preprints, 2nd Symposium Toward a Global Earth Observation System of Systems - Future National Operational Eviron. Satellite Systems*, Atlanta, GA, Amer. Meteor. Soc., CD-ROM P2.2.

Goodman, S. J., D. E. Buechler, P. D. Wright, and W. D. Rust, 1988: Lightning and precipitation history of a microburst-producing storm. *Geophys. Res. Lett.*, **15**, 1185–1188.

Goodman, S. J. and Coauthors, 2005: The North Alabama Lightning Mapping Array: Recent severe storm observations and future prospects. *Atmos. Res.*, **76**, 423–437.

Koshak, W. J. and Coauthors, 2004: North Alabama Lightning Mapping Array (LMA): VHF source retrieval algorithm and error analysis. *J. Atmos. Ocean. Tech.*, **21**, 543–558.

Lakshmanan, V., T. Smith, K. Hondl, G. J. Stumpf, and A. Witt, 2006: A real-time, three dimensional, rapidly updating, heterogeneous radar merger technique for reflectivity, velocity and derived products. *Wea. and Forecasting*, **21**, 802–823.

Lakshmanan, V., T. Smith, G. J. Stumpf, and K. Hondl, 2007: The warning decision support system - integrated information. *Wea. and Forecasting*, **22**, 596–612.

Lang, T. J. and Coauthors, 2004: The Severe Thunderstorm Electrification and Precipitation Study (STEPS). *Bull. Amer. Meteorol. Soc.*, **85**, 1107–1125.

MacGorman, D. R., D. W. Burgess, V. Mazur, W. D. Rust, W. L. Taylor, and B. C. Johnson, 1989: Lightning rates relative to tornadic storm evolution on 22 May 1981. *J. Atmos. Sci.*, **46**, 221–250.

McCaul, E. W., 1987: Observations of the hurricane "Danny" tornado outbreak of 16 August 1985. *Mon. Wea. Rev.*, **115**, 1206–1223.

McCaul, E. W., J. Bailey, S. J. Goodman, R. Blakeslee, and D. E. Buechler, 2005: A flash clustering algorithm for North Alabama Lightning Mapping Array data. *Preprints, Conf. on Meteorological Applications of Lightning Data*, San Diego, CA, Amer. Meteor. Soc., CD-ROM, 5.2.

McCaul, E. W., Jr., 1991: Buoyancy and shear characteristics of hurricane-tornado environments. *Mon. Wea. Rev.*, **119**, 1954–1978.

Petersen, W. A., H. J. Christian, and S. A. Rutledge, 2005: TRMM observations of the global relationship between ice water content and lightning. *Geophys. Res. Lett.*, **32**, doi:10.1029/2005GL023236.

Rison, W., R. J. Thomas, P. R. Krehbiel, T. Hamlin, and J. Harlin, 1999: A GPS-based three dimensional lightning mapping system: Initial observations in central New Mexico. *Geophys. Res. Lett.*, **26**, 3573–3576.

Saunders, C. P. R., W. D. Keith, and R. P. Mitzeva, 1991: The effect of liquid water on thunderstorm charging. *J. Geophys. Res.*, **96**, 11 007–11 017.

Steiger, S. M., R. E. Orville, and L. D. Carey, 2007: Total lightning signatures of thunderstorm intensity over North Texas. Part I: Supercells. *Mon. Wea. Rev.*, **135**, 3281–3302.

Steiger, S. M., R. E. Orville, M. J. Murphy, and N. W. S. Demetriades, 2005: Total lightning and radar characteristics of supercells: Insights on electrification and severe weather forecasting. *Preprints, Conf. on the Meteor. Appl. of Lightning Data*, San Diego, CA, Amer. Meteor. Soc., P1.7.

Takahashi, T., 1978: Riming electrification as a charge generation mechanism in thunderstorms. *J. Atmos. Sci.*, **35**, 1536–1548.

Tessendorf, S. A., L. J. Miller, K. C. Wiens, and S. A. Rutledge, 2005: The 29 June 2000 supercell observed during STEPS. Part I: Kinematics and microphysics. *JAS*, **62**, 4127–4150.

Tessendorf, S. A., K. C. Wiens, and S. A. Rutledge, 2007: Radar and lightning observations of the 3 June 2000 electrically inverted storm from STEPS. *Mon. Wea. Rev.*, **135**, 3665–3681.

Vonnegut, B., 1963: Some facts and speculation concerning the origin and role of thunderstorm electricity. *Severe Local Storms, Meteor. Monogr.*, Amer. Meteor. Soc., 224–241.

Wiens, K. C., S. A. Rutledge, and S. A. Tessendorf, 2005: The 29 June 2000 supercell observed during steps. Part II: Lightning and charge structure. *J. Atmos. Sci.*, **62**, 4151–4177.

Williams, E. R., 1985: Large scale charge separation in thunderclouds. *J. Geophys. Res.*, **90**, 6013–6025.

Williams, E. R., 1989a: The tripole structure of thunderstorms. *J. Geophys. Res.*, **94**, 13 151–13 167.

Williams, E. R. and Coauthors, 1999: The behavior of total lightning activity in severe Florida thunderstorms. *Atmos. Res.*, **51**, 245–265.

Workman, E. J. and S. E. Reynolds, 1949: Electrical activity as related to thunderstorm cell growth. *Bull. Amer. Meteor. Soc.*, **30**, 142–144.

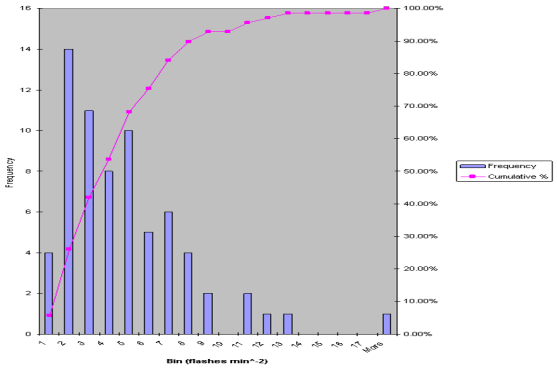

FIG. 1. Presented here is the histogram of 69 non-severe thunderstorm DFRDT rates (flashes min^{-2}). The 90% level is near 8 flashes min^{-2} and the 93% level is near 10 flashes min^{-2}.

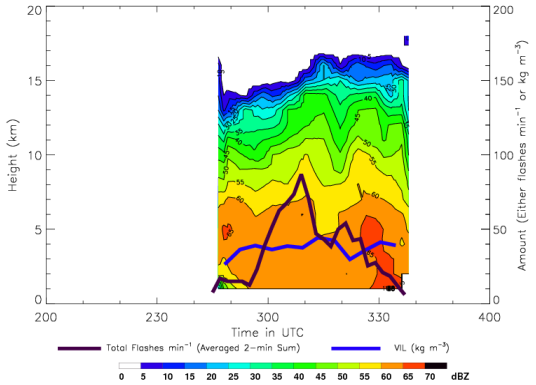

FIG. 2. Presented here is the time-height plot from Thunderstorm A using reflectivity data from KHTX on April 4, 2007. Reflectivity contours are every 5 dB, total flash rate (flashes min^{-1}) is represented by the solid purple line, and the solid blue line represents VIL (kg m^{-3}). The merge with the MCS occurred between 0300 and 0310 UTC, and was identified by the increase in the total flash rate and in 35 dBZ echo top height. The analysis period ends when the individual cell that is being tracked falls below the -15°C height.

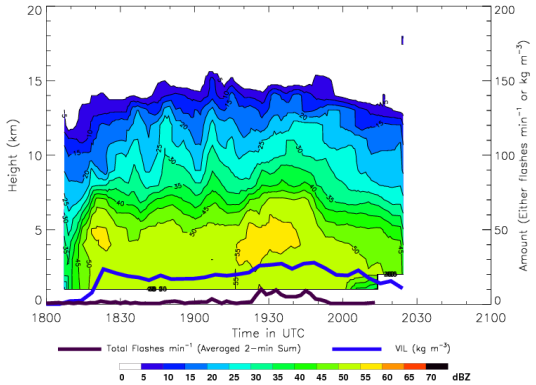

FIG. 3. Represented here is the time-height plot from Thunderstorm A using reflectivity data from KBMX on September 25, 2005. Total flash rate (flashes min^{-1}) is represented by the solid purple line, and the solid blue line represents VIL (kg m^{-3}). A strong reflectivity core developed just before there is an increase in the total flash rate between 1923 and 1927 UTC. Around this same time 35 dBZ echo tops increased from 8 to 9 km.

TABLE 1. Number of False Alarms for Non-Severe Convection

	Gatlin	2σ	3σ	Threshold 10	Threshold 8
No. of False Alarms	92	16	10	6	7

TABLE 2. Results for the Gatlin Algorithm with a 30 minute warning length.

	POD	FAR	CSI	HSS
Within 100 km				
Severe only	0.8922	0.4204	0.5417	0.7027
Severe and Non-Severe	0.8922	0.6286	0.3555	0.5245
Within 150 km				
Severe only	0.8984	0.4912	0.4812	0.6497
Severe and Non-Severe	0.8984	0.6384	0.3474	0.5157

TABLE 3. Results for the Gatlin Algorithm with a 45 minute warning length.

	POD	FAR	CSI	HSS
Within 100 km				
Severe only	0.9804	0.5780	0.5714	0.6497
Severe and Non-Severe	0.9804	0.6169	0.3802	0.5510
Within 150 km				
Severe only	0.9766	0.4726	0.5208	0.6849
Severe and Non-Severe	0.9766	0.6201	0.3765	0.5470

TABLE 4. Results for the 2σ algorithm with a 45 minute warning length.

	POD	FAR	CSI	HSS
Within 100 km				
Severe only	0.8725	0.2583	0.6692	0.8018
Severe and Non-severe	0.8725	0.3456	0.5973	0.7479
Within 150 km				
Severe only	0.8984	0.2813	0.6647	0.7986
Severe and Non-Severe	0.8984	0.3466	0.6085	0.7566

TABLE 5. Results for the 3σ algorithm with a 45 minute warning length.

	POD	FAR	CSI	HSS
Within 100 km				
Severe only	0.4902	0.1803	0.4425	0.6135
Severe and Non-severe	0.4902	0.2958	0.4065	0.5780
Within 150 km				
Severe only	0.5156	0.1646	0.4681	0.6377
Severe and Non-Severe	0.5156	0.2584	0.4681	0.6083

TABLE 6. Results for the Threshold 10 Algorithm with a 45 minute warning length.

	POD	FAR	CSI	HSS
Within 100 km				
Severe only	0.7353	0.2991	0.5597	0.7177
Severe and Non-severe	0.7353	0.3363	0.5357	0.6977
Within 150 km				
Severe only	0.7578	0.3264	0.5543	0.7132
Severe and Non-Severe	0.7578	0.3533	0.5359	0.6978

TABLE 7. Results for the Threshold 8 algorithm with a 45 minute warning length.

	POD	FAR	CSI	HSS
Within 100 km				
Severe only	0.8039	0.3387	0.5694	0.7257
Severe and Non-severe	0.8039	0.3740	0.5430	0.7039
Within 150 km				
Severe only	0.8281	0.3653	0.5608	0.7186
Severe and Non-Severe	0.8281	0.3908	0.5408	0.7020